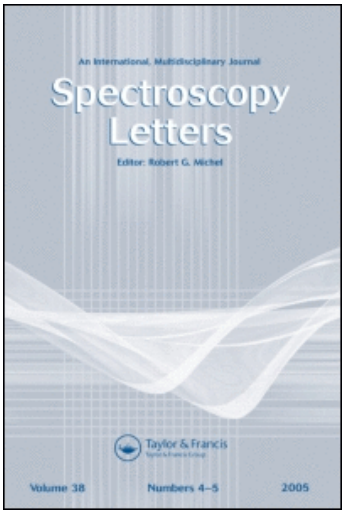

Spectroscopy Letters
Publication details, including instructions for authors and subscription information:
http://www.informaworld.com/smpp/title~content=t713597299

Synthesis and Structural Chemistry of 2,4-Dinitrosoresorcionl, 1-Nitroso-2-naphthol and 4-Carboxy-2-nitrosophenol

M. S. Masoud[a]; A. M. Hindawey[a]; M. A. Mostafa[b]; A. M. Ramadan[a]
[a] Chemistry Dept., Faculty of Science, Alex. University, Alex, Egypt [b] Chemistry and Physics Dept., Faculty of Education, Alex University, Alex, Egypt

To cite this Article Masoud, M. S. , Hindawey, A. M. , Mostafa, M. A. and Ramadan, A. M.(1997) 'Synthesis and Structural Chemistry of 2,4-Dinitrosoresorcionl, 1-Nitroso-2-naphthol and 4-Carboxy-2-nitrosophenol', Spectroscopy Letters, 30: 7, 1227 — 1247
To link to this Article: DOI: 10.1080/00387019708006720
URL: http://dx.doi.org/10.1080/00387019708006720

SPECTROSCOPY LETTERS, 30(7), 1227-1247 (1997)

SYNTHESIS AND STRUCTURAL CHEMISTRY OF 2,4-DINITROSORESORCIONL, 1-NITROSO-2-NAPHTHOL AND 4-CARBOXY-2-NITROSOPHENOL

M.S. Masoud; A.M. Hindawey*; M.A. Mostafa** and A.M. Ramadan**
* Chemistry Dept., Faculty of Science Alex. University, Alex., Egypt.
** Chemistry and Physics Dept., Faculty of Education Alex. University,Alex., Egypt.

ABSTRACT

The stereochemistry of iron, cobalt, nickel and copper complexes derived from 2,4-dinitrosoresorcinol, 1-nitroso-2-naphthol and 4-carboxy-2-nitrosophenol was studied based on elemental analysis and spectral (UV-visible and IR) measurements. More information are obtained on their structures by means of differential thermal analysis (DTA) and electrical conductivity measurements. Empirical equations are deduced for the conduction of the ligands and their metal complexes. The thermodynamic parameters of thermal decomposition are evaluated. Detailed Mössbauer spectra were recorded for the iron complexes.

INTRODUCTION

In view of the role played by nitroso complexes in body systems, delineation of the nature of the metal binding and the stereochemistry in nitroso complexes seems to be interesting[1]. In our laboratory, there has been an escalating popularity interest for the potential nitroso family complexes[2-16]. The major interests of this paper are: (i) the synthesis of the ligands and their complexes, (ii) assigning the stereochemistry of the complexes based on spectroscopic measurements and elemental analysis, (iii) throw light on the mechanism of the electrical conductivity of the ligands and their metal complexes and relate the mechanism to their physico-chemical properties, (iv) study the thermal behaviour of some of these complexes to throw more light on the solid state reactions present, (v) more information are obtained on the structure of the iron complexes from Mössbauer spectral measurements.

EXPERIMENTAL

(i) Synthesis of the ligands:

The metal-free compounds were prepared by the usual nitrosation of the appropriate phenol[17]. These are 2,4-dinitrosoresorcinol (DNR), 1-nitroso-2-naphthol (NBN) and 4-carboxy-2-nitrosophenol (CNP).

(ii) Synthesis of transition metal complexes:

Iron, cobalt, nickel and copper complexes of the nitroso ligands were prepared by mixing the required weights of the metal chloride salts with the corresponding ligand in aqueous alcoholic media. The formed compounds were filtered, washed several times with alcohol and dried in a vacuum desiccator over P_4O_{10}. The metal content was determined using the usual complexometric titration procedure[18,19]. The nitrogen content was analysed by the usual Kjeldahl technique[19]

(iii) Spectral measurements:

The KBr disc infrared spectra of the ligands and their complexes were measured over the range 200-4000 cm^{-1}.

The nujol mull[20] spectrophotometric measurments in the visible and ultraviolet regions were made with Perkin-Elmer spectrophotometer model lambda 4B covering the wavelength range 190-900 nm.

(iv) Conductivity measurements:

Electrical conductivities were measured in the temperature range 249 to 423°K. The samples were prepared in the form of tablets at a pressure of 4 tons/cm^2. The tablets were of an area 1.37 cm^2 and 0.12 mm thickness. The samples were hold between two copper electrodes with silver paste in between and then inserted with the holder vertically into a cylindrical electric furnace. Both ends of the furnace were closed off to reduce drafts. The potential drop across the heater was varied gradually through variac transformer to produce a slow rate of the increase of temperature to get accurate temperature measurements. The circuit used to measure the electrical conductivity consists of d.c. regulated power supply Heath Kit (0-400 volts), Keithley multimeter for measuring current with a sensitivity up to 10^{-15} amp. The temperature of the sample was measured within ±0.1 degree by means of copper-constant thermocouple. The conductivity of the sample was obtained in the case of cooling using the general equation:

$$\sigma = I\, d / V_c\, a$$

where I is the current in ampere, V_c is the potential drop across the sample of the cross-section area "a" and thickness "d".

(v) Thermal analysis:

It was performed on Du pont 9900 computerized thermal analyzer. 60 mg sample was placed in a platinum crucible. Dry nitrogen was flowed over the sample at a rate 10 cc/min and a chamber cooling water flow rate was 10 l/h. The speed was 5 mm/min. The heating rate of the DTA was 10 degree/min.

(vi) Mössbauer spectra:

Such spectra were recorded at room temperature using a computerized Mössbauer spectrometer MS-1200, model: Ranger, in standard transmission geometry and with a 20 mCi Co^{57} (Rh) source. Mössbauer spectra have been analyzed by means of least square computer

fitting using Mössfit computer program. The isomer shift values refer to that of metallic iron at room temperature.

RESULTS AND DISCUSSION

Stoichiometry of the complexes

The prepared complexes are with variable stoichiometries, 1:1, 1:2 and 1:3, (M:L), Table (1). The reaction[21] of 1-nitroso-2-naphthol,HL, with cobalt (II) chloride afforded the formation of CoL_3 complex accompanied by reduction of the ligand and oxidation of Co^{II} to Co^{III}. Such reaction was represented as follows:

$$2\ CoCl_2 + 7\ HL \rightarrow 2\ CoL_3 + H_2O + 4\ HCL + \text{Organic products}$$

On the other hand, the reaction of 1-nitroso-2-naphthol, HL, with iron (III) chloride gave two complexes with different stoichiometries [1:2(FeL_2) and 1:3(FeL_2HL)], via partial reduction of Fe^{III} to Fe^{II}.

Fe^{III} gave 1:3 complexes with 2,4-dinitrosoresorcinol and 4-carboxy-2-nitrosophenol, H_2L. The following equation is proposed to represent such reaction:

$$Fe^{III} + 3\ H_2L \rightarrow Fe(HL)_3 + 3\ H^+$$

The interaction of the prepared nitroso ligands with some transition metal salts to give 1:2 complexes is proposed in the following equations:

$$M^{II} + 2\ HL \rightarrow ML_2 + 2\ H^+$$

HL: 1-nitroso-2-naphthol — M: Ni, Cu

$$M^{II} + 2H_2L \rightarrow M(HL)_2 + 2H^+$$

H_2L: 2,4-dinitrosoresorcinol — M: Co,Ni

However, the interaction of 2,4-dinitrosoresorcinol, H_2L, with copper (II) chloride afforded the formation of a 1:1 complex as follows:

$$CuCl_2 + H_2L \rightarrow CuCl(HL) + HCl$$

Most of these complexes, Table (1), possess some sorts of water.

Characterization of the complexes

Infrared studies:

The IR spectra of the prepared nitroso ligands and their metal complexes gave multiplet bands in the region 3800-2350 cm^{-1}, due to ν_{OH} & $\nu_{C\text{-}H}$ involving intra- or intermolecular hydrogen bonding. The elemental analysis, (Tables 1), typified an interaction between the water molecules and the host complexes [e.g. Fe-NBN (1:2); ($FeL_2.6H_2O$), Co-DNR; ($Co(HL)_2.6H_2O$)]. However, the broad ν_{OH} nature of the other complexes with no water is due to the existence of an internal hydrogen bond[22]. The medium to strong bands at 1465, 1480 and 1550 cm^{-1} in CNP are due to ν_{NO}. Such bands are strongly affected in the presence of Fe^{III} due to complex formation where the nitroso group is involved in such structure. For the

Table (1): Analytical data for metal complexes.

Complex	Stoichiometry	Formula	% calculated (% found)	
			M	N
Co-DNR	(1:2).6H_2O	$C_{12}H_{18}N_4O_{14}Co$	11.8 (12.1)	11.2 (11.2)
Co-NBN	1:3	$C_{30}H_{18}N_3O_6Co$	10.3 (9.9)	7.3 (7.2)
Fe-NBN	1:3	$C_{30}H_{19}N_3O_6Fe$	9.7 (9.4)	7.3 (7.4)
Fe-NBN	(1:2). 6H_2O	$C_{20}H_{24}N_2O_{10}Fe$	11.0 (11.0)	5.5 (5.2)
Fe-DNR	1:3	$C_{18}H_9N_6O_{12}Fe$	10.0 (10.3)	15.1 (15.3)
Ni-DNR	(1:2). 2H_2O	$C_{12}H_{10}N_4O_{10}Ni$	13.7 (14.0)	13.1 (13.1)
Ni-NBN	(1:2). 2H_2O	$C_{20}H_{16}N_2O_6Ni$	13.4 (12.9)	6.4 (6.7)
Cu-DNR	(1:1). 6H_2O	$C_6H_{15}N_2ClO_{10}Cu$	17.0 (17.3)	7.5 (7.1)
Cu-NBN	(1:2) 4H_2O	$C_{20}H_{20}N_2O_8Cu$	13.3 (13.3)	5.8 (5.3)

All the complexes with melting points > 270 °C.

simplest nitrosobenzene, two strong bands were recorded at 1490 and 850 cm^{-1} assigned to ν_{NO} and δ_{NO}, respectively[23]. However, the latter band appeared as a doublet band at 830 and 775 cm^{-1} for CNP compound. The abnormal behaviour in this region for the 4-carboxy compound illustrates its existence in an associated structure through hydrogen bond[23].

The NO group may be bonded through nitrogen, or oxygen. The presence of more than a structure through resonance and chelate ring formation leads to extra stability:

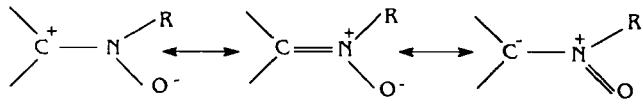

The polarizing effect of the metal ions affects the π-electrons of the aromaticity of the ligands. On complexation with the metal ion, nitroso-nitrogen is favoured than nitroso-oxygen, due to stability effect where a chelate structure is formed[24].

DNR was previously studied from coordination and analytical chemistry views[5,6]. The free ligand gave four well defined IR bands at 3520 (ν_{OH} of oxime), 3400 (ν_{OH} of phenolic -OH), 3180 and 2750 cm^{-1}. The latter two bands are for hydrogen bonded -OH groups. The bands at 1700, 1660, 1600 and 965 cm^{-1} indicated the presence of oxime structure with a resonance possessing intramolecular hydrogen bonding[25] accompanied by the possible existence of cis and trans isomers[3,5], (I) and (II), respectively:

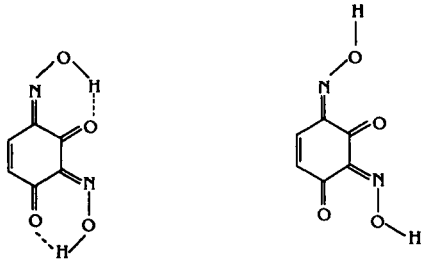

(I) (II)

On comparing the infrared spectra of the DNR ligand to that of its complexes, Table (2), the medium ν_{NO} band at 1380 cm^{-1} in the ligand becomes in the range 1350-1390 cm^{-1} with strong feature on complexation, probably due to the increase in bond polarity through conjugation[26]. So, the nitroso group is complexed, with a differ in the strength of the M-NO bond from a complex to the other. The δ_{NO} band within the range 830-870 cm^{-1} in the complexes favoured the nitrosophenol structure. Meanwhile, the $\nu_{C=O}$ band of the ligand is not highly affected on complexation, to suggest that half of the ligand is probably existing in the oxime structure and the second is in the nitrosophenol tautomer.

NBN exists in different tautomeric equilibria[27], with a broad carbonyl band and a lack of bands to hydroxyl absorption. So, The oxime structure is proposed rather than the nitrosophenol. The strong band in the region 1640-1580 cm^{-1} in the free ligand assigned to $\nu_{C=N}$ overlapped with $\nu_{C=O}$. The strong feature is due to the increase in the bond polarity owing to conjugation in the naphthalene nucleus[26]. However, this region in the free ligand is strongly affected on complexation where the C=O bands are absent and that due to $\nu_{C=N}$ is shifted to lower wave number. This leads to suggest that the ligand is acquired the nitrosophenol structure rather than the oxime tautomer on complexation. Such finding is further supported where the strong band located at 965 cm^{-1}, in the free ligand due to ν_{NOH} becomes absent on complexation.

Electronic spectra studies:

The greenish black Fe-DNR and the brown Fe-CNP complexes gave a band of broad nature with band maximum near 730 and 720 nm, respectively, due to dynamic Jahn-Teller effect or from static tetragonal D_{4h} distortion of the primary coordination sphere. Such band is due to the $^5E_{2g} \rightarrow {}^5T_{2g}$ transition to assign octahedral spatial configuration[28]. However, the two dark green iron complexes with different stoichiometries FeL_2HL and $FeL_2.6H_2O$, (HL=NBN), showed a distinct band at 455 nm beside a broad absorption band in the wavelength range 658-777 nm. Such data assigned the existence of pseudooctahedral iron (II) complexes resulting from $^5T_{2g} \rightarrow {}^5E_g$ transition[29]. The intense dark green colour of these complexes is probably an indication to the appearance of charge-transfer bands in the visible region[30]. This is consistent with the better π-acceptor properties of the naphthalene ring[31]. Both (1:3)

Table (2): Fundamental infrared bands (cm^{-1}) of DNR and its complexes.

Compound	νOH	νNOH	νC=O	νC=N	δNO	νNO
DNR	3520 (s) 3400 (s) 3180 (b) 2750 (b)	965 (s)	1700 (s) 1660 (s)	1600 (s)	855 (m)	1380 (m)
Cu-DNR	3430 (b) 2630 (w)	945 (s)	1665 (s) 1620 (s)	1570 (s)	840 (m)	1370 (s)
Ni-DNR	3445 (b) 3140 (b)	940 (s)	1660 (s) 1630 (s)	1570 (s)	835 (m)	1350 (s)
Co-DNR	3430 (b) 3160 (w)	940 (m)	1665 (s) 1630 (s)	1570 (s)	830 (m)	1380 (s)
Fe-DNR	3430 (b) 3140 (w)	970 (w)	1655 (s) 1625 (s)	1565 (s)	870 (w)	1390 (s)

Fe-NBN and (1:2) Fe-NBN complexes are of great similarity from the IR and electronic spectral views.

The nujol mull electronic spectra of the dark brown cobalt (II) complex, Co-DNR, showed a band at 460 nm assigned to $^4T_{1g}(F) \rightarrow {}^4T_{1g}(P)$ and diagnostic of an octahedral geometry[32]. However, the two electronic spectral bands of the cobalt (III) complex, Co-NBN, at 550 and 420 nm assigned to $^1A_{1g} \rightarrow {}^1T_{1g}$ and $^1A_{1g} \rightarrow {}^1T_{2g}$ transitions, respectively, diagnostic of regular octahedral structure[33].

The band at 390 nm in the nujol mull electronic spectra of Ni-DNR complex, $Ni(HL)_2.2H_2O$, could be assigned to an octahedral spatial configuration where the water molecules are in the inner sphere. This is probably due to the spin-allowed transition: $^3A_{2g} \rightarrow {}^3T_{1g}$ (P). However, a well characterized broad band appeared in the wavelength range 420-500 nm in the electronic spectra of the Ni^{II} complex with NBN due to the existence of more than d-d transition overlapped with each other[34] reflecting the octahedral geometry.

The strong band at 450 nm in the electronic spectra of the Cu^{II} complex with DNR, $CuCl(HL).6H_2O$, is a strong indication to the presence of a square planar stereochemistry mainly of $^2B_{1g} \rightarrow {}^2B_{2g}$ electronic transition in D_{4h} symmetry[35]. The nature of the ligand and the stoichiometry of this complex pinpoint to the existence of square planar geometry with bidentate attachment through nitrogen atom of the NO group and the phenolic oxygen of one of the two OH groups. The chloride content was found to be 9.1% using oxygen flask method[19], indicating the presence of one Cl^- in the coordination sphere. The fourth coordination number around the copper (II) center can be achieved via coordinated water molecule and/or copper-copper bond. Since, the spectral data lack a band around 370-375 nm, the Cu-Cu interaction can be ruled out. The electronic spectra of Cu^{II} with NBN, $CuL_2.4H_2O$ showed bands of broad nature with band maximum at 420 and 500 nm. Such data are in harmony with (SPY) geometry,

(550-670 nm)[36]. The transitions occur at higher energy in the ultraviolet region, (420 and 550 nm), probably due to existence of charge transfer from the metal to a low-lying vacant π^*-antibonding orbital of the naphthalene moiety[31]. Elemental analysis (Table 1), infrared and electronic spectral data suggest the following structures of the compounds:

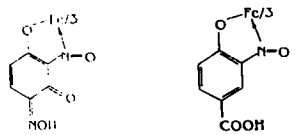

$Fe(HL)_3$

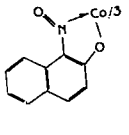

CoL_3

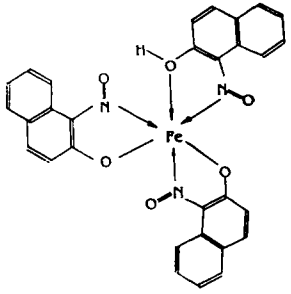

$FeHL(L_2)$

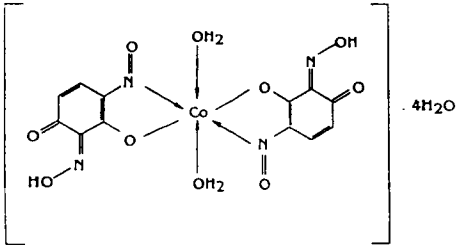

$Co(HL)_2.6H_2O$

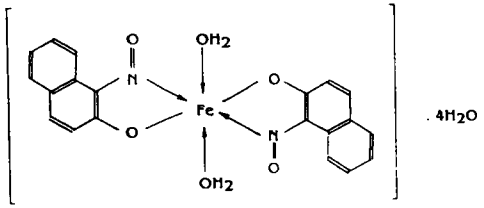

$FeL_2.6H_2O$

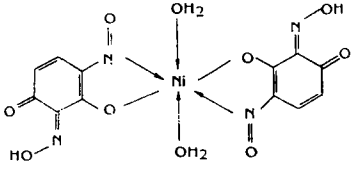

$Ni(HL)_2.2H_2O$

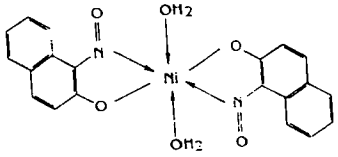

$NiL_2.2H_2O$

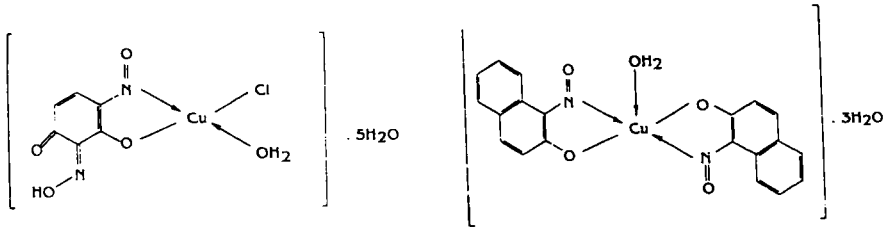

$CuCl(HL).6H_2O$ $CuL_2.4H_2O$

Electrical conductivity measurements:

The temperature dependence of the electrical conductivity of the ligands (DNR and NBN) and their metal complexes obeys the following equation[37]:

$$\sigma = \sigma_0 \exp \frac{-\Delta E}{KT}$$

where σ and ΔE are the specific conductivity and the activation energy, respectively. σ_0 is a pre-exponential term, K Boltzmann constant. The ΔE and log σ_0 values are evaluated and correlated, Tables (3,4). The data point to the semiconducting trend of the systems under investigation. The log σ- 1/T relationship for the metal-free ligands gives the following comments:

(1) Both DNR and NBN free ligands proceed in a similar manner where the conductivity curves showed more than one straight line intersect with each other at a characteristic transition temperature (Four regions: A, B, C and D). The regions A, C and D are with a positive temperature coefficient of electrical conductivity but negative in B.

(2) The region B, is characterized by the decrease of conductivity as the temperature increased. This results of scattering of carriers by photons, due to lattice vibrations within the temperature range, [DNR (41.5-98.7°C), NBN (44.5-111.6°C)], covering this region[38].

(3) The region A exhibits an increase of conductivity as the temperature is increased with a relatively low activation energy, [DNR (0.070 eV), NBN (0.187 eV)], due to the activation from the donor level to the conduction band i.e. an extrinsic behaviour. However, regions C and D have a positive temperature coefficient with an activation energy higher than that of region A, [DNR (0.209,0.722 eV), NBN (0.224,0.714 eV)], this assigns an intrinsic region of conductivity, where the conduction is from the valence band to the conduction band [38].

On dealing with the electrical conductivity properties of the metal complexes compared with their metal-free ligands (DNR & NBN), the following could be deduced:

(1) The magnitudes of the conductivities of the ligands and their metal complexes favour assignment to a faint semiconducting behaviour rather than metallic conductors, or that promotion of electrons from ground to excited states may be necessary before

Table(3): Electrical conductivity data of DNR and its complexes.

Compound	Region	ΔE (eV)	log σ_o ($ohm^{-1}cm^{-1}$	Transittion temperature (°K)
DNR	A	0.070	-8.588	314.5
	B	-0.186	-12.700	371.7
	C	0.209	-7.330	460.8
	D	0.722	-1.698	
Ni-DNR	A	0.109	-7.350	312.5
	B	-0.146	-11.475	365.0
	C	0.269	-5.718	487.8
	D	1.503	7.070	
Fe-DNR	A	0.183	-4.730	333.3
	B	-0.283	-11.311	377.4
	C	-0.731	-16.679	421.9
	D	1.203	4.246	467.3
Cu-DNR	A	0.681	3.217	330.0
	B	-0.821	-19.794	353.4
	C	0.256	-4.394	
Co-DNR	A	0.495	0.680	333.3
	B	-1.044	-22.647	369.0
	C	-0.177	-10.775	429.2
	D	0.489	-2.926	

Table (4): Electrical conductivity data of NBN and its complexes.

Compound	Region	ΔE (eV)	log σ_o ($ohm^{-1}cm^{-1}$	Transittion temperature (°K)
NBN	A	0.187	-5.962	317.5
	B	-0.237	-12.715	384.6
	C	0.224	-6.655	465.1
	D	0.714	-1.329	
Ni-NBN	A	0.594	2.025	312.5
	B	0.180	-4.661	380.2
	C	-0.396	-11.920	411.5
	D	0.352	-3.647	456.6
Fe-NBN (1:2)	A	0.163	-4.750	352.1
	B	-0.225	-10.311	456.6
	C	0.873	1.846	
Fe-NBN (1:3)	A	0.107	-4.296	339.0
	B	-0.059	-6.764	373.1
	C	-0.583	-13.869	442.5
	D	0.940	3.503	
Cu-NBN	A	0.853	6.224	331.1
	B	-0.910	-20.692	354.6
	C	0.233	-4.394	
Co-NBN	A	0.198	-3.460	331.1
	B	0.037	-5.921	363.6
	C	0.178	-3.955	

conduction occurs. Hence, the electrons in the available orbitals of the complexes are not of high mobility.

(2) For all the complexes, the electrical conductivity increases and the activation energy decreases on going from the free ligand to its metal complexes. So, the metal ion can act as a bridge to facilitate the flow of the current [39].

(3) The discontinuity in the conductivity curves of the metal-free ligands is retained in their metal chelate complexes where log σ - 1000/T relationship showed three or four segments with variable activation energies, Tables(3,4), probably due to different crystallographic or phase transitions[40-42].

(4) The Ni-NBN and Fe-DNR complexes reveal no change in conductivity with increasing temperature within the temperature range, [(107.2-138.5°C), (60.3-104.4°C)] respectively, to be of an insulator properties under these conditions.

(5) The region C has a positive temperature coefficient in all complexes similar to metal-free ligands (except for Co-DNR, Fe-DNR, Ni-NBN and (1:3) Fe-NBN (Tables 3,4), probably as a result of scattering of carriers by photons, due to lattice vibrations within the temperature range covering this region[38].

(6) The region B has a negative temperature coefficient in all complexes similar to metal-free ligands [except for Ni-NBN and Co-NBN, where an increasing of conductivity occurs with temperature with low activation energy, (0.180, 0.037 eV respectively), probably due to activation from the donor level to the conduction band i.e. an extrinsic behaviour][38].

(7) The conductivity data given in Tables (3,4) clearly indicated that the complexing properties affected the values of the transition temperatures for their corresponding ligands. The transition temperatures lie within the temperature range 40-110°C [e.g. Cu-NBN (58.1°C), Co-DNR (60.3°C) and Ni-DNR (92°C)] may be attributed to the drop in the resistivity of the ligands (which might be due to the replacement of hydrogen atoms with the metal atoms), or the dehydration of the complex. However, the transition temperatures lie up to 120°C are due to the lattice defect of the dehydrated complex, [e.g. Co-DNR (156.2°C), Ni-DNR (214.8°C)][38].

(8) The ΔE values for the (1:2) and (1:3) Fe-NBN complexes decrease as the molecular weight increases, Table (4), i.e. the iron content in the prepared complex controls the conductivity behaviour of the complex. The magnitudes of conductivities for the (1:3) Fe-NBN complex are higher than those of the (1:2) Fe-NBN complex. This might be due to distortions in the conduction pathways through the metal caused by lattice imperfections which affect the movement of electrons. Therefore, the delocalization of electrons within the metal-atom chains play some role[43].

The straight line relation of ΔE versus log σ_0 assists the deduction of empirical equations based on least square method of calculations as follows:

$\Delta E_i = 0.082 \log \sigma_i^o + 0.800$ for DNR & NBN ligands
$\Delta E_i = 0.088 \log \sigma_i^o + 0.641$ for iron complexes
$\Delta E_i = 0.066 \log \sigma_i^o + 0.476$ for cobalt complexes
$\Delta E_i = 0.085 \log \sigma_i^o + 0.685$ for nickel complexes
$\Delta E_i = 0.066 \log \sigma_i^o + 0.480$ for copper complexes

The mobilities, μ, of the ligands and their metal complexes are calculated based on the equation, $\sigma = eN_o\mu$, where N_o is the number of current carriers, ($N_o = 10^{21}$). The values of μ are in the range 7.5×10^{-9}-4.23×10^{-13} $cm^2V^{-1}sec^{-1}$. The fact that these values are much smaller than 1 $cm^2V^{-1}sec^{-1}$ can be used as a criterion for applying the "hopping model" for the description of the mechanism of conductance. Therefore the charge carrier passes to another molecule over the top of the barrier via an excited state(44).

Thermal studies:

The DTA data of the prepared cobalt, iron, nickel and copper complexes of DNR (H_2L) and NBN (HL) ligands are given in Tables (5,6). The octahedral Co-NBN complex, CoL_3 gave a horizontal line extending upto 579°K showing its great stability upto this temperature. The decomposition of the complex occurs in two subsequent steps: i) in the temperature range 579-668°K, ii) in the temperature range 668-728°K corresponding to the oxidation of the organic matter and ends with the formation of a stable product CoO(45).

The DTA data of Fe-NBN complexes: FeL_2HL and $[FeL_2(H_2O)_2].4H_2O$, Table (5), are of great similarity with two exceptions:

i) The O_h $[FeL_2(H_2O)_2].4H_2O$ complex gave three DTA peaks at 395.6, 495.2 and 674.4°K with activation energies of 83.7, 654.6 and 209.4 KJ/mole, respectively. However, the O_h FeL_2HL complex gave only two peaks at 484.4 and 657.2°K with activation energies of 783.4 and 400.7 KJ/mole, respectively. The difference in the data can be attributed to the presence of two coordinated water molecules and four water molecules in the outersphere in the former complex. So, the first broad peak within the temperature range 372.9-449.7°K in this complex can be assigned to a dehydration process.

ii) The higher E_a values of the first and second decomposition steps for the FeL_2HL complex compared to the second and third decomposition steps in $[FeL_2(H_2O)_2].4H_2O$ complex is probably due to the presence of three NBN ligands in its complex, to reflect its high thermal stability. The similarity of the DTA curves of both complexes above 470°K suggested that both decomposed in the same manner, i.e. end with the same decomposition products (like Fe_2O_3)(46).

The O_h Fe-DNR complex, $Fe(HL)_3$, gave three successive DTA peaks at 440.1, 495.2 and 605.4°K with activation energies 487.4, 270.2 and 323.6 KJ/mole accompanied with order of reactions 1.11, 1.37 and 1.45, respectively, Table (5). These peaks could be assigned to thermal agitation followed by material decomposition for the complex ended with the formation of metal oxide(46).

Table (5): Thermal properties of cobalt and iron complexes of DNR and NBN ligands.

Complex	T_m/°K	E_a/$K_J mol^{-1}$	n	α_m	$\Delta S^{\#}$/$K_J K^{-1} mol^{-1}$	$\Delta H^{\#}$/$K_J mol^{-1}$	Z/sec^{-1}	Assignment
Co-NBN	600.8	481.9	2.22	0.480	-0.226	-135.8	18.9	Decomposition of the complex
	683.5	431.5	2.14	0.487	-0.230	-157.2	14.1	Oxidation of organic matter, forming of CoO
Fe-NBN	484.4	783.4	1.16	0.605	-0.217	-105.1	48.4	Decomposition of the complex
(1:3)	657.2	400.7	2.44	0.462	-0.230	-151.2	13.7	Loss of rest of ligand and formation of Fe_2O_3
Fe-NBN	395.6	83.7	1.83	0.517	-0.235	-93.0	4.52	Loss of $4H_2O$ outersphere molecules, loss
(1:2)								of 2 coordinated H_2O molecules
	495.2	654.6	1.35	0.576	-0.219	-108.4	36.5	Decomposition of the complex
	674.4	209.4	1.57	0.547	-0.236	-159.2	6.58	Loss of rest of ligand and formation of Fe_2O_3
Fe-DNR	440.1	487.4	1.11	0.613	-0.220	-96.8	30.0	Thermal agitation
	495.2	270.2	1.37	0.573	-0.228	-112.9	12.5	Material decomposition of the complex
	605.4	323.6	1.45	0.562	-0.230	-139.2	11.9	Formation of Fe_2O_3

Table (6): Thermal properties of nickel and copper complexes of DNR and NBN ligands.

Complex	T_m/°K	E_a/KJmol^{-1}	n	α_m	$\Delta S^{\#}$/KJK^{-1}mol^{-1}	$\Delta H^{\#}$/KJmol^{-1}	Z/sec^{-1}	Assignment
Ni-NBN	441.4	13.2	1.36	0.574	-0.252	-111.2	0.60	Loss of 2 coordinated H_2O molecules
	605.6	590.9	1.01	0.630	-0.224	-135.7	23.7	Decomposition of the complex
	643.4	643.7	1.49	0.557	-0.225	-144.8	24.2	Material decomposition, forming of NiO
Cu-NBN	359.0	39.4	0.98	0.636	-0.240	-86.2	2.28	Loss of 3 outersphere H_2O molecules and one coordinated H_2O molecule
	507.0	829.6	1.26	0.411	-0.217	-110.0	48.4	Decomposition of the complex
	656.0	744.4	1.26	0.411	-0.224	-146.9	28.0	Formation of CuO
Ni-DNR	469.1	629.1	1.44	0.563	-0.218	-102.3	37.9	Thermal agitation, loss of 2 coordinated H_2O molecules
	552.6	131.9	1.39	0.570	-0.237	-131.0	5.04	Decomposition of the complex
	628.6	362.2	1.37	0.573	-0.230	-144.6	12.9	Material decomposition, forming of NiO
Cu-DNR	405.0	54.7	1.29	0.584	-0.239	-96.8	2.82	Loss of 5 outersphere H_2O molecules
	461.5	789.9	1.26	0.411	-0.215	-99.2	53.6	Loss of one coordinated Cl and one coordinated H_2O
	577.0	165.8	1.50	0.556	-0.235	-135.6	6.12	Decomposition of the complex
	731.5	423.9	1.14	0.608	-0.231	-169.0	12.8	Fromation of $CuCl_2$
	746.3	446.3	1.06	0.621	-0.231	-172.4	13.2	Formation of CuO

The DTA data of O_h nickel complexes, [Ni-NBN, $[NiL_2(H_2O)_2]$ and Ni-DNR, $[Ni(HL)_2(H_2O)_2]$], Table (6), showed that both complexes gave three exothermic DTA peaks. The first peaks are at 441.4 and 469.1°K for the $[NiL_2(H_2O)_2]$ and $[Ni(HL)_2(H_2O)_2]$ complexes, respectively, due to the loss of the two coordinated water molecules with activation energies 13.2 and 629.1 Kj/mole, respectively. The large E_a for the Ni-DNR complex may be due to strong thermal agitation accompanying the water elimination. This probably points to the existence of the complex in an associated structure through intermolecular hydrogen bonding network and/or intramolecular hydrogen bonding between the coordinated water and the host molecule(47).

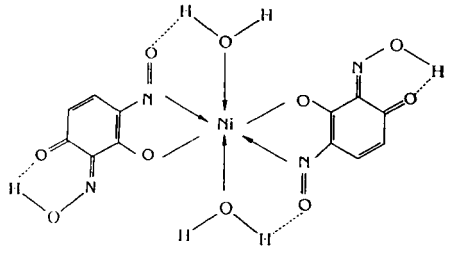

15.

Ni-DNR

The second and third peaks of the Ni-NBN, $NiL_2(H_2O)_2$[605.6°K, 643.4°K] & Ni-DNR, $Ni(HL)_2(H_2O)_2$ [552.6°K, 628.6°K] complexes, Table (6), may be assigned to the decomposition steps ended with the formation of NiO as a final product(45). Based on the E_a values of these peaks, Table (6), the following order is observed:

$$E_a \text{ of Ni-DNR} < E_a \text{ of Ni-NBN}$$

Both complexes have the same stoichiometry and the same geometry (O_h). The greater π-acceptor properties of NBN ligand with electron sink nature of the naphthalene nucleus permits the π-back donation of electrons from the metal ion to the coordinating groups leading to increase the bond order of the groups bonded to the metal ion. Such scope results in much more stability of the NBN complex(31) compared to the DNR complex. This trend goes in harmony with comparison the E_a values of [Fe-NBN (1:3), Fe-DNR] and [Cu-NBN, Cu-DNR] pairs, Tables (5,6).

The square pyramidal Cu-NBN complex, $[CuL_2(H_2O)].3H_2O$, gave three DTA peaks. The first peak at 359°K within the temperature range 314-386°K corresponds to the dehydration process, with activation energy 39.4 Kj/mole and an order of 0.98, i.e. of the first order type. However, other decomposition steps corresponding to the oxidation of the complex and

formation of CuO as a final residue[48], appeared as exothermic peaks at 507°K and 656°K, Table (6).

The square planar Cu-DNR complex, $[Cu(HL)Cl(H_2O)].5H_2O$, showed five decomposition peaks at 405, 461.5, 577, 731.5 and 746.3°K with energies of activation 54.7, 789.9, 165.8, 423.9 and 446.3 KJ/mole, respectively, accompanied with the decomposition orders 1.29, 1.26, 1.50, 1.14 and 1.06, respectively, Table (6). The first broad endopeak at 405°K is due to dehydration process of the outersphere water molecules within the temperature range 371-450°K. The broad nature of the DTA peak suggests that the loss of the five outersphere water molecules occurs in more than one stage. The strong second exothermic peak at 461.5°K is probably due to an overlapping process of two steps (loss of the one coordinated H_2O molecule and decomposition of Cu-Cl bond)[46]. The last three DTA peaks could be assigned to decomposition steps of the complex ended with the formation of CuO[45]. Generally, two patterns of behaviour can be discerned[49]: i) the chloro complex with the metal decomposed directly to the oxide, ii) it decomposed endothermically to the metal chloride followed by an exothermic conversion to the oxide. The datum is in harmony with the second pattern where an endothermic peak appeared at 731.5°K assigned to the formation of copper chloride followed by an exothermic one at 746.3°K due to the formation of copper oxide.

The change of entropy, $\Delta S^{\#}$, values for all complexes, Tables (5,6), are nearly of the same magnitude and lie within the range -0.215 to -0.252 $KJ\ K^{-1}\ mole^{-1}$. So, the transition states are more ordered, i.e. in a less random molecular configuration, than the reacting complexes. The fraction appeared in the calculated order of the thermal reactions, n, Tables (5,6), also confirmed that the reactions proceeded in complicated mechanisms. The calculated values of the collision number, Z, Tables (5,6), showed a direct relation to E_a.

A well noticeable observation is recorded for nitroso complexes where some explosion occurs to explain the high values of energy of activation in many DTA peaks, Tables (5,6). This is probably due to complicated decomposition of such complexes and oxidation of the organic matter with the formation of different products, e.g. nitrogen oxides (NO, NO_2), metal oxides, organic products.

The position of the peak is defined by the peak temperature, T_m, at which the peak maximum or minimum occurs. The values of the decomposed substance fraction, α_m, at maximum development of the reaction was calculated from the equation[50]:

$$(1-\alpha_m) = n^{\frac{1}{1-n}}$$

It is of nearly the same magnitude and lies within the range 0.411 - 0.636.

In general, the change in enthalpy ($\Delta H^{\#}$) for any phase transformation taking place at any peak temperature, T_m, can be given by the following equation:

$$\Delta S^{\#} = \frac{\Delta H^{\#}}{T_m}$$

where $\Delta S^{\#}$ is the entropy of activation calculated from the following equation[51]:

$$Z = \frac{K\,Tm}{h} \exp\left(\frac{\Delta S^{\#}}{R}\right)$$

The values of Z were obtained in case of Horowitz-Metzger[52] by making use of the relation:

$$Z = \frac{E}{R\,Tm}\phi \exp\left(\frac{E}{R\,T_m^2}\right)$$

where, R represents molar gas constant, ϕ rate of heating (Ks^{-1}), K the Boltzmann constant and h the Planck's constant.

Mössbauer studies:

The M ssbauer data of the prepared iron complexes are collected in Table (7). The Mössbauer parameters of Fe-CNP complex displayed a doublet spectral lines (ΔE_Q = 0.615, δ= 0.366 mm/sec.), Figure (1). These parameters are consistent with those for high spin Fe^{III} complexes[53]. The obtained isomer shift value (δ = 0.366, mm/sec.) is lower than those reported for high spin Fe^{III} complexes (δ ~ 0.5 -0.7 mm/sec.)[54], probably due to the increase in the electron density at the nucleus or due to the increasing in covalency character of the bond between the iron (III) atom with the π-acceptor NO group of the ligand. Such covalency promotes d-electron transfer from the non-δ-bonding orbitals of the central atom to π-acceptor orbitals of the ligand with appropriate symmetry. Such electron transfer results in an increase in the symmetry of the d shell owing to the spherically symmetric d^5 electron structure ($t_{2g}^3\ e_g^2$) characteristic of the high-spin iron (III) atom. The symmetry of the charge distribution around the iron nucleus results in a decrease in the electric field gradient at the position of the nucleus. This in turn leads to a decrease in the quadrupole splitting (ΔE_Q = 0.615 mm/sec.).

The Mössbauer parameters for the complexes: Fe-DNR, (1:3) Fe-NBN and (1:2) Fe-NBN, Figures (2-4), are collected in Table (7). These complexes gave two bands, each of doublet nature to assign the presence of high-spin iron (III) and low-spin iron (II)[54]. The

Table (7): Mössbauer parameters for iron nitroso-complexes.

Complex	δ ($mm.s^{-1}$)	ΔE_Q ($mm.s^{-1}$)	Fe^{II}/Fe^{III}
Fe-CNP	Fe^{III} 0.366	0.615	-
Fe-DNR	Fe^{III} 0.405 Fe^{II} 0.210	0.720 0.750	0.583
Fe-NBN (1:3)	Fe^{III} 0.345 Fe^{II} 0.075	0.840 0.780	1.155
Fe-NBN (1:2)	Fe^{III} 0.405 Fe^{II} 0.180	0.720 0.750	1.174

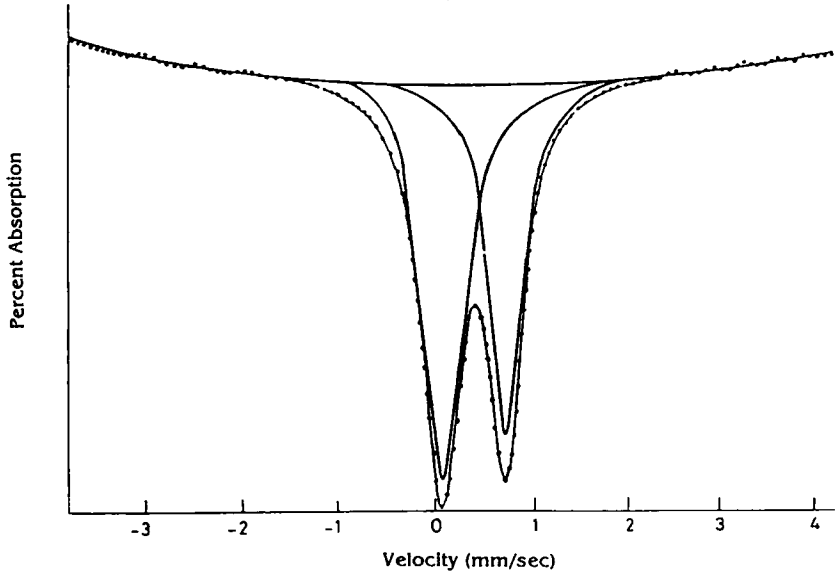

Figure (1): Mössbauer spectrum of Fe-CNP

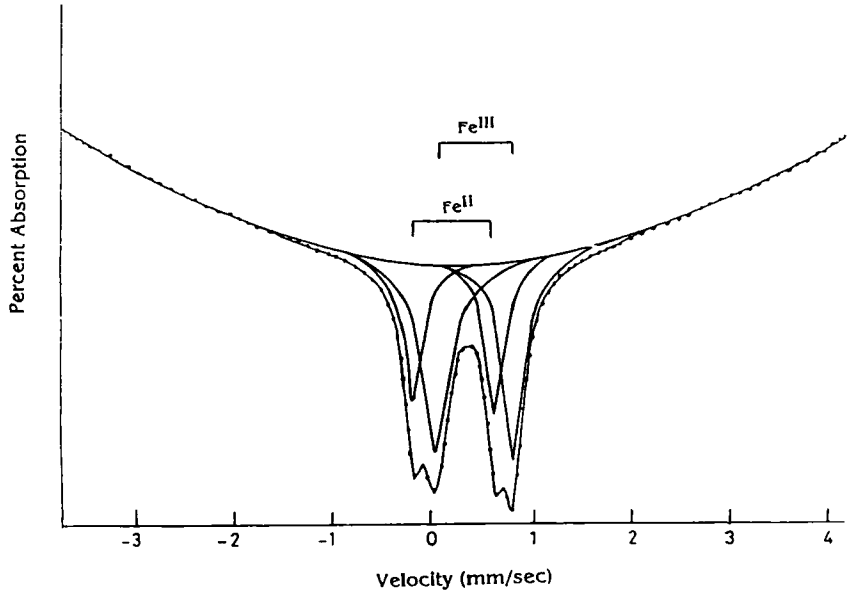

Figure (2): Mössbauer spectrum of Fe-DNR

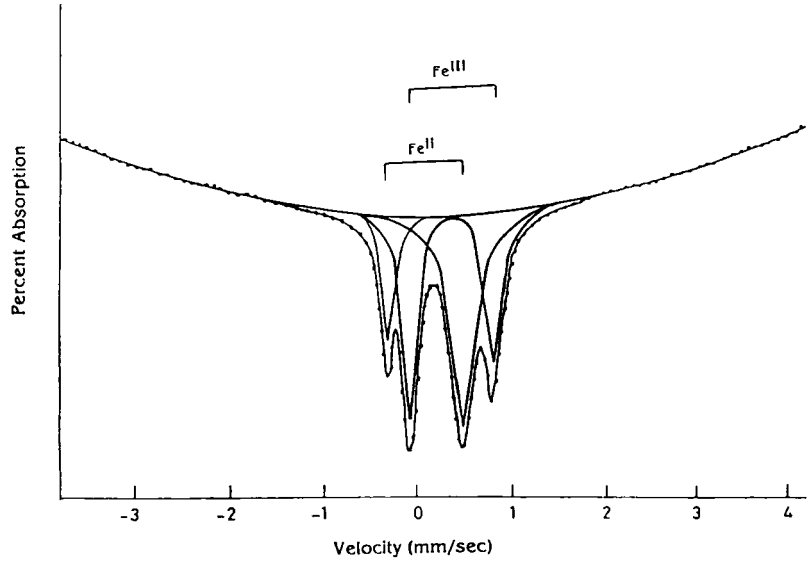

Figure (3): Mössbauer spectrum of Fe-NBN (1:3)

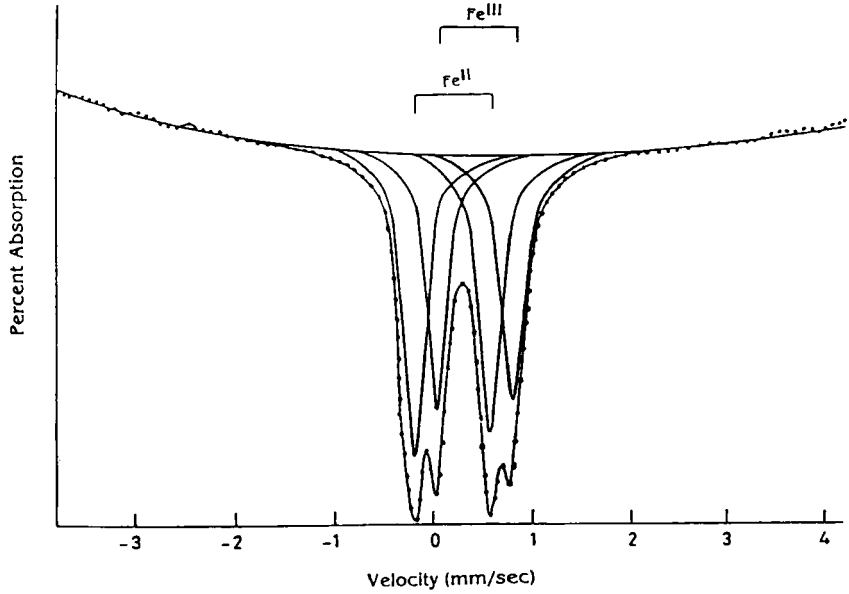

Figure (4): Mössbauer spectrum of Fe-NBN (1:2)

contribution of Fe^{II} and Fe^{III} in the same molecule exists in the ratio (Fe^{II}/Fe^{III}): 0.583, 1.155 and 1.174, respectively, in the above three complexes. Such ratio is calculated from the total area of the peaks of each iron state, (Fe^{II}, Fe^{III}). Such data go in concordance with μ_{eff} value of the (1:3) Fe-NBN complex. The μ_{eff} value (3.12 B.M. at 303°K) is lower than those of h.s. and higher than those of l.s. of typical octahedral iron complexes. The asymmetric doublet spectral lines may be due to the superposition of a singlet transition from a low spin iron (II) and a quadrupole doublet from a high-spin iron (III). Such results are in agreement with those obtained from the Mössbauer spectra of Prussian blue[55]. The latter compound gave an asymmetric doublet due to the superposition of a singlet transition from the ferrocyanide and a quadrupole doublet from the high-spin iron (III). There is little or no transfer of enriched iron to the low-spin species.

These observations lead to suggest the occurrence of a partial reduction of the iron during the progress of complexation of iron salt with the nitroso ligands. In general, it seems from the Fe^{II}/Fe^{III} ratios that Fe^{II} is highly contributed in case of NBN complexes, while in case of DNR complex, the Fe^{III} is predominant.

Also, the lower δ values than a typical high spin iron (III) and a low spin iron (II) reflect the covalency between the metal ions and the π-acceptor NO group. Moreover, the quadrupole splitting of the signals reveals the asymmetry of the electric field surrounding the metal centers[54].

REFERENCES

1. C.L. Walters, *Chemistry in Britain*, **13**, 140 (1977).
2. M.S. Masoud; A.M. Khalil and I. Abd. El-Gawad, *Indian J. Chem.*, **15**, 468 (1977).
3. M.S. Masoud; M.M. Osman and H. El-Naggar, *Z. Anal. Chem.*, **289**, 207 (1978).
4. M.S. Masoud and S.A. Ghonaim, *Polish J. Chem.*, **54**, 651 (1980).
5. M.S. Masoud; T.M. Salem and M. El-Essawi, *Synth. React. Inorg. Metorg. Chem.*, **13**, 79 (1983).
6. M.S. Masoud; B.S. Farag; Y. Sawan; T.M. Salem and M. El-Essawi, *J. Non-Crystalline Solids*, **55**, 209 (1983).
7. M.S. Masoud; A. El-Dessouky and S.S. Haggag, *Spect. Lett.*, **18**, 251 (1985).
8. M.S. Masoud; A. El-Dissouky and E.E. Ghatwary, *Trans Met. Chem.*, **11**, 161 (1986); *Polyhedron*, **5**, 1867 (1986); *Inorg. Chim. Acta*, **141**, 119 (1988).
9. M.S. Masoud; M. El-Essawi and A.M. Amr, *Reviews in Inorg. Chem.*, **19**, 253 (1988).
10. M.S. Masoud; Z. Zaki and F.M. Ismail, *Thermochim. Acta*, **156**, 225 (1989).
11. M.S. Masoud; S.S. Haggag and S. Abou El-Enein, *Delta J. Sci*, **14**, 1511 (1990).
12. M.S. Masoud; A. El-Dissouky; F.A. Aly and S. Abou El-Enein, *Trans. Met. Chem.*, **14**, 443 (1990).
13. M.S. Masoud; A.M. Hindawy; A. El-Dissouky; G.B. Mohamed and T.M. Abd El-Fattah, *Trans. Met. Chem.*, **16**, 181 (1991).
14. M.S. Masoud; A. El-Dissouky; H.M. El-Nahas and E.E. Ghatwary, *Polish J. Chem.*, **65**, 49 (1991).
15. M.S. Masoud and S.S. Haggag, *Thermochim. Acta*, **196**, 221 (1992).
16. M.S. Masoud; O.H. Abd El-Hamid and Z.M. Zaki, *Trans. Met. Chem.*, **19**, 21 (1994).
17. A.I. Vogel, "*A Text Book of Practical Organic Chemistry*", Third Edition, Longman, London (1962).

18. G. Schwarzenbach "*Complexometric Titration*", Translated by H. Irving, Metheun Co., London (1959).
19. A.I. Vogel, "*A Text Book of Quantitative Inorganic Analysis*", Third Edition, Longman, London (1964).
20. R.H. Lee; E. Griswold and J. Kleinberg, *Inorg. Chem.*, **3**, 1278 (1964).
21. J. Charalambous; G. Soobramanien; A. Betts and J. Bailey, *Inorg. Chim. Acta*, **60**, 151 (1982).
22. S. Satapathy and B. Sahoo, *J. Inorg. Nucl. Chem.*, **32**, 2223 (1970).
23. W. Lüttke, *J. Phys. Radium.*, **15**, 633 (1954).
24. A.T. Pilipenko; L.L. Shevophenko; J.A. Pavalova and V.V. Trachevskü, *Khim. Teknol.*, **23**, 939 (1980).
25. M.M. Aly; M. Makhyoun and S.El-Ezaby, *J. Inorg. Nucl. Chem.*, **35**, 2727 (1973).
26. K. Nakamoto and R.E. Rundle, *J. Am. Chem. Soc.*, **78**, 1113 (1956).
27. S. Gurrieri and G. Siracusa, *Inorg. Chim. Acta*, **5**, 650 (1971).
28. J.G. Bailer; H.J. Emdens; R. Nyholm and A.F.T. Dickenson, *"Comprehensive Inorganic Chemistry"*, Vol. 3, p. 1043 (1973).
29. B.F. Little and G.J. Long, *Inorg. Chem.*, **17**, 3401 (1978).
30. J.S. Haynes; A. Kostikas; J.R. Sams; A. Simopoulos and R.C. Thompson, *Inorg. Chem.*, **26**, 2630 (1987).
31. A.B.P. Lever; J. Lewis and R.S. Nyholm, *J. Chem. Soc.*, 4761 (1964).
32. A.B.P. Lever and D. Ogden, *J. Chem. Soc. A*, 2041 (1967).
33. F.A. Cotton "*Advanced Inorganic Chemistry*", Third Edition, Wiley Eastern limited, London (1979).
34. B.T. Thaker and P.K. Battacharya, *Indian J. Chem.*, **14**, 619 (1976).
35. A.A.G. Tomlinson and B.J. Hathaway, *J. Chem. Soc. A*, 2578 (1968).
36. B.J. Hathaway; I.M. Procter; R.C. Slade and A.A.G. Tomlinson, *J. Chem. Soc. A*, 2219 (1969).
37. D.C. Olson; V.P. Mayweg and G.N. Schrauzer, *J. Am. Chem. Soc.*, **88**, 4876 (1966).
38. M.S. Masoud; S. Abou El-Enein and E.El-Shereafy, *J.Therm.* Anal., **37**, 365 (1991)
39. T.M. Salem; M.M. Osman; M.S. Masoud; M.F.El-Shazly and M.M. Abou Sekkina, *Al-Physica*, **2**,43 (1979).
40. M.S. Masoud; E. El-Shereafy; E.A. Khalil and O.H. Abd El-Hamid, *Egypt J. Chem.*, **2**, 95 (1993).
41. M.S. Masoud; M.S. Tawfik and M.E. El-Shabasy, *Bull. Fac. of Sci.*, El-Minia Univ., **6**, 67 (1993).
42. S. Abou El-Enein; M.S. Masoud; A. El-Khatib and S. Abd El-Aziz, *Alex. Engin. J.*, **33**, D 103 (1994).
43. M.S. Masoud; E.M. Soliman and M.E.El-Shabasy, *Thermochim. Acta*, **125**, 9 (1988).
44. S.H. Glarum, *J. Phys. Chem. Solids*, **24**, 1577 (1963).
45. A.M. Gadalla and H.F. Yu, *J. Therm. Anal.*, **37**, 319 (1991).
46. S.L. Stefan, *J. Therm. Anal.*, **42**, 1299 (1994).
47. M.S. Masoud; A.M. Donia and S. Abou El-Enein, *Thermochim. Acta*, **161**, 217 (1990).
48. D.M. Petrovic; A.F. Petrovic, V.M. Leovac and S.R. Lukic, *J. Therm. Anal.*, **41**, 1165 (1994).
49. J.R. Allan; B. McCloy and A.D. Paton, *Thermochim. Acta.*, **214**, 211 (1993).
50. H.R. Oswald and E. Dubler, "*Thermal Analysis*", Edited by H.G. Wiedemann, Volume 2, Switzerland (1972).
51. M.L. Dhar and O.Singh, *J. Therm. Anal.*, **37**, 259 (1991).
52. H. Horowitz and G. Metzger, *Anal. Chem.*, **35**, 1464 (1963).

53. D.P. Riley; P.H. Merrell; J.A. Stone and D.H.Busch, *Inorg. Chem.*, **14**, 490 (1975).
54. S.J.Lippard and J.M. Berg, "*Principles of Bioinorganic Chemistry*", University Science Books, Mill Valley, California, P. 91 (1994).
55. K.Maer; M.L. Beasley; R.L. Collins and W.O. Milligan, *J.Am. Chem. Soc.*, **90**, 3201 (1968).

Date Received:November 21, 1996
Date Accepted:April 15, 1997